Available online at www.sciencedirect.com

ScienceDirect

Green Energy & Environment xxx (xxxx) xxx

www.keaipublishing.com/gee

Research paper

C_2H_2 semi-hydrogenation on the Pd_xM_y cluster/graphdiyne catalysts: Effects of cluster composition and size on the activity and selectivity

Ying Wang [a,1], Yamin Qi [a,1], Maohong Fan [b,c,d,*], Baojun Wang [a], Lixia Ling [a], Riguang Zhang [a,**]

[a] *Key Laboratory of Coal Science and Technology of Ministry of Education and Shanxi Province, Taiyuan University of Technology, Taiyuan, 030024, Shanxi, PR China*
[b] *Departments of Chemical and Petroleum Engineering, University of Wyoming, Laramie, 82071, WY, USA*
[c] *School of Civil and Environmental Engineering, Georgia Institute of Technology, Atlanta, 30332, GA, USA*
[d] *School of Energy Resources, University of Wyoming, Laramie, 82071, WY, USA*

Received 15 July 2020; revised 14 September 2020; accepted 20 October 2020
Available online ■ ■ ■

Abstract

C_2H_2 semi-hydrogenation has been widely applied in industry to eliminate trace C_2H_2 from C_2H_4 feed. C_2H_2 semi-hydrogenation to C_2H_4 on a series of the newly designed catalysts, graphdiyne (GDY) as a new carbon allotrope supported different sizes of Pd_xM_y clusters (Pd_xM_y/GDY, M = Cu, Ag, Au, Ni; x+y = 1−3), were studied using DFT calculations. The results found that C_2H_2 semi-hydrogenation to C_2H_4 on Pd_xM_y/GDY catalysts exhibits that both the activity and selectivity greatly depend on the composition and size of Pd_xM_y/GDY catalysts. Surprisingly, our results for the first time discovered the Pd_1/GDY catalyst with GDY supported the single atom Pd that presents the best selectivity and activity toward C_2H_4 formation compared to the previously reported catalysts so far in C_2H_2 semi-hydrogenation. This study would provide a theoretical clue for designing and screening out the potential catalysts with GDY supported small sizes of Pd_xM_y and other metal clusters in C_2H_2 hydrogenation.

Keywords: Acetylene; Semi-hydrogenation; Graphdiyne; Cluster size; Cluster composition

1. Introduction

C_2H_2 semi-hydrogenation to C_2H_4 is a commonly used method to remove small quantity of C_2H_2 impurities in C_2H_4-rich stream, in which C_2H_2 acts as an impurity that poisons the catalysts used subsequently for the polymerization of ethylene [1–3]. In C_2H_2 semi-hydrogenation, the most effective catalyst was found to be Pd-based catalysts owing to high C_2H_2 conversion occurred at low temperature, however, C_2H_4 selectivity still needs to be improved because of C_2H_4 over-hydrogenation to ethane [4–6]. Thus, the development of Pd-based catalysts with high selectivity and activity in C_2H_2 semi-hydrogenation is still highly expected.

Nowadays, in order to effectively utilize the active components of the catalyst, the metal catalyst is usually dispersed on the support with high specific surface area. However, only a small part of surface metal atoms participate in the catalytic reaction and the atom utilization rate is low. Thus, small size of supported metal clusters have been reported due to high atom utilization and more unique catalytic performance, however, the particle size in the subnanometer range is sensitive to its structure with particular electronic properties. For example, Liu et al. [7] theoretically found that the size of Pd_n clusters affects H_2 dissociation activity on

---

* Corresponding author. Departments of Chemical and Petroleum Engineering, University of Wyoming, Laramie, 82071, WY. USA.
** Corresponding author.
E-mail addresses: mfan@uwyo.edu, mfan3@mail.gatech.edu (M. Fan), zhangriguang@tyut.edu.cn (R. Zhang).

[1] Y. W. and Y. Q. contributed equally to this work.

https://doi.org/10.1016/j.gee.2020.10.020

Please cite this article as: Y. Wang et al., C_2H_2 semi-hydrogenation on the Pd_xM_y cluster/graphdiyne catalysts: Effects of cluster composition and size on the activity and selectivity, Green Energy & Environment, https://doi.org/10.1016/j.gee.2020.10.020

Pd_n(n = 4,6,13,19,55) clusters. Mercedes et al. [8] calculated the LUMO and HOMO orbitals of Au_1~Au_{38} clusters, and predicted that Au_1, Au_3 and Au_{38} have the best activity. Zhang et al. [9] prepared the atomically dispersed Pt_3 clusters anchored over the core−shell nanodiamond@graphene, which presented excellent catalytic performance for n-butane direct dehydrogenation at a temperature as low as 450 °C. On the other hand, for C_2H_2 semi-hydrogenation, Gluhoi et al. [10] observed that when Au particle size was less than 3 nm, Au/Al_2O_3 showed high C_2H_2 conversion and C_2H_4 selectivity. Abdollahi et al. [11] found that Pd_2 cluster have higher activity than Pd_{12} cluster, indicating that Pd_2 cluster is more suitable. Density functional theory (DFT) studies by Xiao et al. [12] found that H_2 adsorption capacity on the graphene supported Pd_n(n = 1−5) clusters was stronger than that on Pd (111) surface. Huang et al. [13] prepared single atom Cu catalyst supported by the nanodiamond-graphene, C_2H_2 conversion is 95%, C_2H_4 selectivity is 98%, and the catalyst has good stability. Shi et al. [14] experimentally synthesized Cu single atom and nanoparticles corresponding to the sizes of about 3.4, 7.3 and 9.3 nm over Al_2O_3 support using atomic layer deposition, indicating that a size decrease of Cu nanoparticle obviously reduces the activity of C_2H_2 semi-hydrogenation but gradually improves both C_2H_4 selectivity and durability. The experiments by Huang et al. [15] prepared Pd_1/ND@G catalyst with the atomically dispersed Pd over a defective nanodiamond-graphene (ND@G), which showed significantly high C_2H_4 selectivity (90%) and C_2H_2 conversion (100%) in C_2H_2 semi-hydrogenation. Thus, the studies on small size of metal cluster presenting particular active sites are of great significance in C_2H_2 semi-hydrogenation.

Recently, graphdiyne (GDY), a new allotrope carbon material including C atoms with sp and sp^2 hybrid, has attracted broad attentions [16–21]. The C atoms of GDY show a π−π conjugate system, which is highly delocalized in the whole planar framework [16,22,23]. Moreover, in comparison with grapheme, GDY has a unique pore structure to provide abundant adsorption site and more open storage space for molecular adsorption. As shown in Fig. 1, the basic geometry of GDY is 6-membered ring (6 MR) and 18-membered ring (18 MR). The 18 MR structure provides a natural framework for anchoring metal clusters through a strong metal carbon covalent bond, thus forming a stable and isolated structure. For example, Lu et al. [24] systematically examined the adsorption of single atom Pd, Pt, Rh or Ir on the GDY, and found that the single atom was favorable for embedding into 18 MR of GDY and combining with four carbon atoms. The adsorption and diffusion behavior of Au, Cu, Fe, Ni or Pt atoms on the GDY were also researched by Lin et al. [25] using theoretical calculation, and found that the metal atoms have good thermal stability and very small overflow rate on the GDY even at 900 K. Chen et al. [26] studied CO oxidation reaction on the GDY supported Ag_{38} cluster, which showed the excellent performance due to the unique combination of the cluster and GDY.

Further, the metal atoms and clusters supported by GDY are also ideal catalysts, which have been widely applied for the hydrogenation reaction of unsaturated hydrocarbons. For example, Xing et al. [27] investigated C_2H_2 semi-hydrogenation over the catalysts with the cluster M_xN_{3-x} (M, N]Ru, Os) supported by GDY, indicating that three atom metal clusters can be firmly anchored on the 18 MR of GDY, and effectively catalyze C_2H_2 semi-hydrogenation to produce C_2H_4; the synergistic effect between the metal cluster and GDY as a charge buffer contributes to the improvement of catalytic performance. However, up to now, few studies about C_2H_2 semi-hydrogenation focus on the catalysts with GDY supported small size of metal clusters Pd_xM_y, meanwhile, the effects of cluster composition and size on the activity and selectivity are still unknown, which would provide an open space for designing highly-efficient GDY supported Pd-based catalyst in C_2H_2 semi-hydrogenation. Moreover, previous studies [28] showed that a Group IB metal (Cu, Ag or Au) doped into Pd to form Pd-based bimetallic alloys can well improve C_2H_4 selectivity in C_2H_2 semi-hydrogenation; meanwhile, Abdollahi et al. [29] theoretically demonstrated that among the Ni_n(n = 2−10) nanoclusters, Ni_6 nanocluster could be used as a suitable catalyst in C_2H_2 semi-hydrogenation. Wongwaranon et al. [30] experimentally observed that C_2H_4 selectivity was improved on the Pd/Ni-modified α-Al_2O_3 catalysts in the presence of Ni atoms. Jin et al. [31] experimentally claimed that PdNi catalyst possessed high selectivity and stability for C_2H_2 semi-hydrogenation. Thus, the bimetallic PdM(M = Cu, Ag, Au, Ni) catalysts can be well applied in C_2H_2 semi-hydrogenation to improve its catalytic performance.

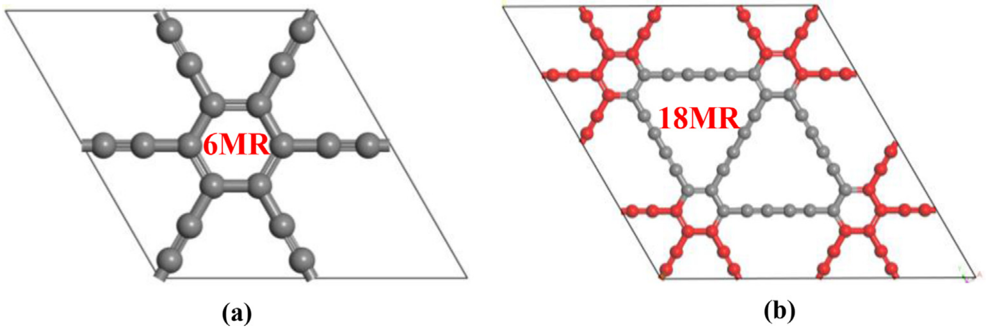

(a) (b)

Fig. 1. The optimized structures for the protocell (a) and the supercell (b) of GDY.

Please cite this article as: Y. Wang et al., C_2H_2 semi-hydrogenation on the Pd_xM_y cluster/graphdiyne catalysts: Effects of cluster composition and size on the activity and selectivity, Green Energy & Environment, https://doi.org/10.1016/j.gee.2020.10.020

In this study, a large number of Pd_xM_y/GDY catalysts using GDY supported different sizes of Pd_xM_y (M = Cu,Ag,Au,Ni; x+y = 1−3) bimetallic clusters have been for the first time designed; Then, the underlying mechanism of the hydrogenation process of C_2H_2 on the Pd_xM_y/GDY catalysts were fully investigated using DFT calculations, the obtained results were expected to illustrate the effects of cluster composition and size in the Pd_xM_y/GDY catalysts on the activity and selectivity of C_2H_4 formation. This study would provide a good clue for designing and screening out the potential catalysts with GDY supported small sizes of Pd_xM_y clusters and other metal clusters in C_2H_2 hydrogenation process.

2. Computational Methods and Models

2.1. Detailed methods

Dmol^3 code [32,33] in Materials Studio 8.0 were carried out for the performance of all DFT calculations. The exchange-correlation functional PBE with generalized gradient approximation (GGA) [34,35] was used. The double-numeric polarized (DNP) basis set was used to expand valence electron functions [36,37]. The van der Waals correction (DFT-D) [38] method was used to correct the weak adsorption free energy underestimated by the GGA functional. The all electron and effective core potential (ECP) basis set were used to treat the non-metal atoms and the inner electrons of metal atoms, respectively [39,40]. The *k*-point 4 × 4 × 1 was considered together with a smearing of 0.005 Ha for all calculations. The complete LST/QST techniques were used to obtain transition state of an elementary step [41,42], which was confirmed by the methods of Frequency analysis and TS confirmation implemented in Dmol^3 code.

A lots of researches showed that the type of active metals [43], the temperature [44] and the H_2/C_2H_2 ratio [45−48] in C_2H_2 semi-hydrogenation can all obviously affect the formation of green oil over Pd-based catalyst, suggesting that the high temperature and high H_2/C_2H_2 ratio can prevent “green oil” formation leading to the deactivation of polymerization catalysts [6,49,50]. This study only focus on the investigations about the effect of the types of active metals including the metal cluster composition and size on the activity and selectivity of C_2H_2 hydrogenation process, as a result, the effect of green oil formation on the activity and selectivity of C_2H_2 hydrogenation process are expected to be ignored, a high temperature of 425 K and a high H_2: C_2H_2 ratio of 10 corresponding to C_2H_4, C_2H_2 and H_2 partial pressures of 0.89, 0.01 and 0.1 atm were performed. Thus, all energies in the process of adsorption and reaction were the values at 425 K in this study (see details in the Supplementary Material).

2.2. The models of Pd_xM_y/GDY catalysts

For the protocell of GDY, see Fig. 1, the C−C bond length on the 6 MR is 1.430 Å, the C−C and CC bond lengths on the 18 MR are 1.390 and 1.232 Å, respectively, which agree with the reported values of 1.430, 1.390 and 1.240 Å [24,51]. For the supercell of GDY, a single-layer *p* (2 × 2) structure with a 30 Å vacuum thickness was constructed, and the lattice constant obtained through structure optimization is 18.880 Å. During the calculations, the edge C atoms of GDY denoted as the red balls in Fig. 1(b) were fixed; the C atoms of two 18 MR were fully relaxed.

For Pd_xM_y/GDY catalysts, as shown in Fig. 2, five types of single metal catalysts, Pd, Cu, Ag, Au and Ni, are used to form metal clusters with the atom numbers of one, two and three, respectively; four types of bimetallic catalysts, Cu, Ag, Au, Ni alloyed with Pd to form Pd_xM_y bimetallic clusters with the atom numbers of two and three, respectively. As a result, there are twenty-seven kinds of Pd_xM_y/GDY catalysts, named as Pd_1/GDY, Pd_2/GDY, Pd_3/GDY, Cu_1/GDY, Cu_2/GDY, Cu_3/GDY, Pd_1Cu_1/GDY, Pd_1Cu_2/GDY, Pd_2Cu_1/GDY, Ag_1/GDY, Ag_2/GDY, Ag_3/GDY, Pd_1Ag_1/GDY, Pd_1Ag_2/GDY, Pd_2Ag_1/GDY, Au_1/GDY, Au_2/GDY, Au_3/GDY, Pd_1Au_1/GDY, Pd_1Au_2/GDY, Pd_2Au_1/GDY, Ni_1/GDY, Ni_2/GDY, Ni_3/GDY, Pd_1Ni_1/GDY, Pd_1Ni_2/GDY and Pd_2Ni_1/GDY, respectively. Further, the interaction between Pd_xM_y cluster and GDY is calculated [52,53] (see details in Table S1).

3. Results and discussion

3.1. Possible routes of C_2H_2 semi-hydrogenation

C_2H_2 semi-hydrogenation follows the continuous hydrogenation of hydrocarbons [54]. Hydrogenation of C_2H_2 may occur by three routes [55−58], as presented in Fig. 3, the first is that C_2H_2(ad) is successively hydrogenated to form C_2H_4(ad) via C_2H_3(ad) intermediate, then, C_2H_4(ad) desorb from the catalyst surface, which is the desired route for C_2H_2 semi-hydrogenation defined as C_2H_4 desorption route. The latter two is that C_2H_2(ad) hydrogenation via the common C_2H_3(ad) intermediate produces C_2H_4(ad) or $CHCH_3$(ad), which could be further hydrogenated to form ethane via C_2H_5(ad) intermediate; these two routes, called as C_2H_4 hydrogenation route and $CHCH_3$ hydrogenation route, are expected to be suppressed to facilitate the semi-hydrogenation of C_2H_2 to form C_2H_4.

For Pd_xM_y/GDY catalysts, to identify whether C_2H_4 desorption route prefers to occur in C_2H_2 semi-hydrogenation, firstly, it is necessary to calculate the priority between C_2H_4 desorption and its hydrogenation, if C_2H_4 desorption is more favored than C_2H_4 hydrogenation, namely, C_2H_4 desorption route is superior to C_2H_4 hydrogenation route; Then, judging whether C_2H_4 desorption route also prefers to occur compared to $CHCH_3$ hydrogenation route. Based on above two aspects of analysis, we can confirm the catalysts with better C_2H_4 selectivity, on which C_2H_4 desorption route is the dominant among three routes.

3.2. The stable configurations of adsorbed C_2H_2 and C_2H_4 species

C_2H_4 feed produced by steam-cracking process is known to contain about 0.1−1% of C_2H_2 [59], only when C_2H_2

Please cite this article as: Y. Wang et al., C_2H_2 semi-hydrogenation on the Pd_xM_y cluster/graphdiyne catalysts: Effects of cluster composition and size on the activity and selectivity, Green Energy & Environment, https://doi.org/10.1016/j.gee.2020.10.020

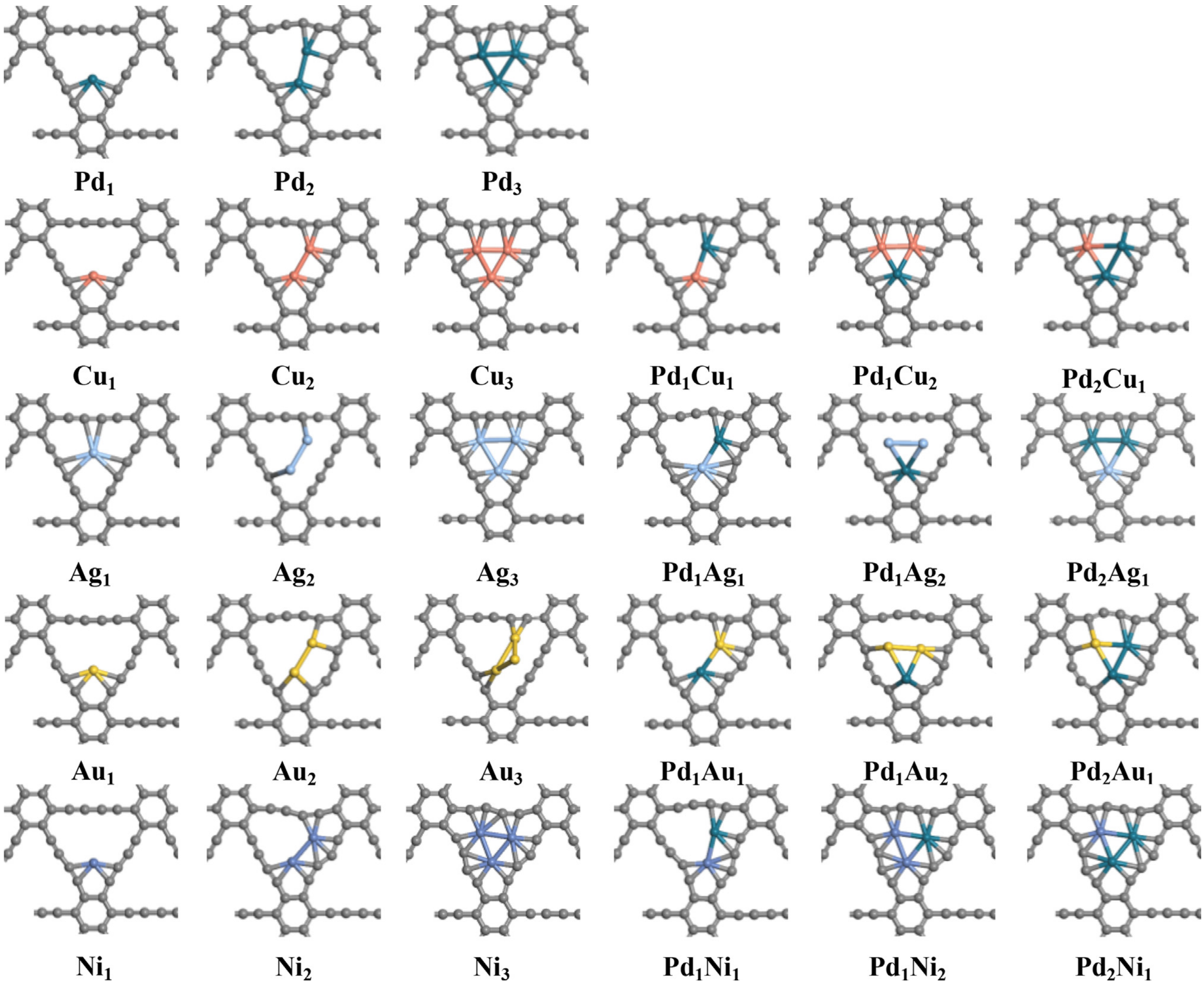

Fig. 2. The optimized structures of Pd_xM_y/GDY (M = Cu, Ag, Au, Ni; x+y = 1–3) catalysts.

adsorption is stronger than C_2H_4 adsorption over the catalysts, the removal of trace C_2H_2 in C_2H_4-rich feed gas could be achieved on the catalysts. The intuitional comparison between C_2H_4 and C_2H_2 adsorption energies on Pd_xM_y/GDY catalysts is shown in Fig. 4 (see details in Table S2 and Fig. S1). For H, C_2H_3, $CHCH_3$ and C_2H_5 species, Fig. S2 and Table S3 give out the adsorption energies and stable configurations on above Pd_xM_y/GDY catalysts.

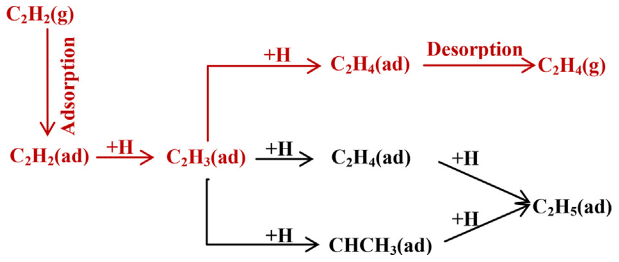

Fig. 3. Three possible routes of C_2H_2 semi-hydrogenation: C_2H_4 desorption route to form gaseous C_2H_4, C_2H_4 hydrogenation route and $CHCH_3$ hydrogenation route to produce C_2H_5. Both (ad) and (g) stand for the adsorbed and gaseous states, respectively.

For Pd_xM_y/GDY catalysts, Ag_3/GDY is seriously deformed and unstable when the C_2H_2 or C_2H_4 species were adsorbed. On the Ag_2/GDY and Ni_3/GDY, C_2H_2 is not effectively adsorbed due to the weak physisoption (4.9 and 8.7 kJ mol^{-1}). On the Ag_1/GDY, Au_1/GDY and Pd_1Au_2/GDY, the adsorption ability of C_2H_2 and C_2H_4 species are close (26.9 and 22.2 kJ mol^{-1}, 125.4 and 129.9 kJ mol^{-1}, 55.2 and 53.9 kJ mol^{-1}), namely, trace C_2H_2 in C_2H_4-rich stream cannot be sufficiently adsorbed. However, as listed in Table S2, C_2H_2 has stronger adsorption ability than C_2H_4 on twenty-one kinds of Pd_xM_y/GDY catalysts, including Pd_1/GDY, Pd_2/GDY, Pd_3/GDY, Cu_1/GDY, Cu_2/GDY, Cu_3/GDY, Pd_1Cu_1/GDY, Pd_1Cu_2/GDY, Pd_2Cu_1/GDY, Pd_1Ag_1/GDY, Pd_1Ag_2/GDY, Pd_2Ag_1/GDY, Au_2/GDY, Au_3/GDY, Pd_1Au_1/GDY, Pd_2Au_1/GDY, Ni_1/GDY, Ni_2/GDY, Pd_1Ni_1/GDY, Pd_1Ni_2/GDY and Pd_2Ni_1/GDY, namely, trace C_2H_2 to participate into the subsequent hydrogenation reaction can be sufficiently adsorbed in C_2H_4-rich stream.

Based on above analysis, six kinds of Ag_3/GDY, Ag_2/GDY, Ni_3/GDY, Ag_1/GDY, Au_1/GDY and Pd_1Au_2/GDY catalysts are excluded in C_2H_2 semi-hydrogenation on the basis of the weak

Please cite this article as: Y. Wang et al., C_2H_2 semi-hydrogenation on the Pd_xM_y cluster/graphdiyne catalysts: Effects of cluster composition and size on the activity and selectivity, Green Energy & Environment, https://doi.org/10.1016/j.gee.2020.10.020

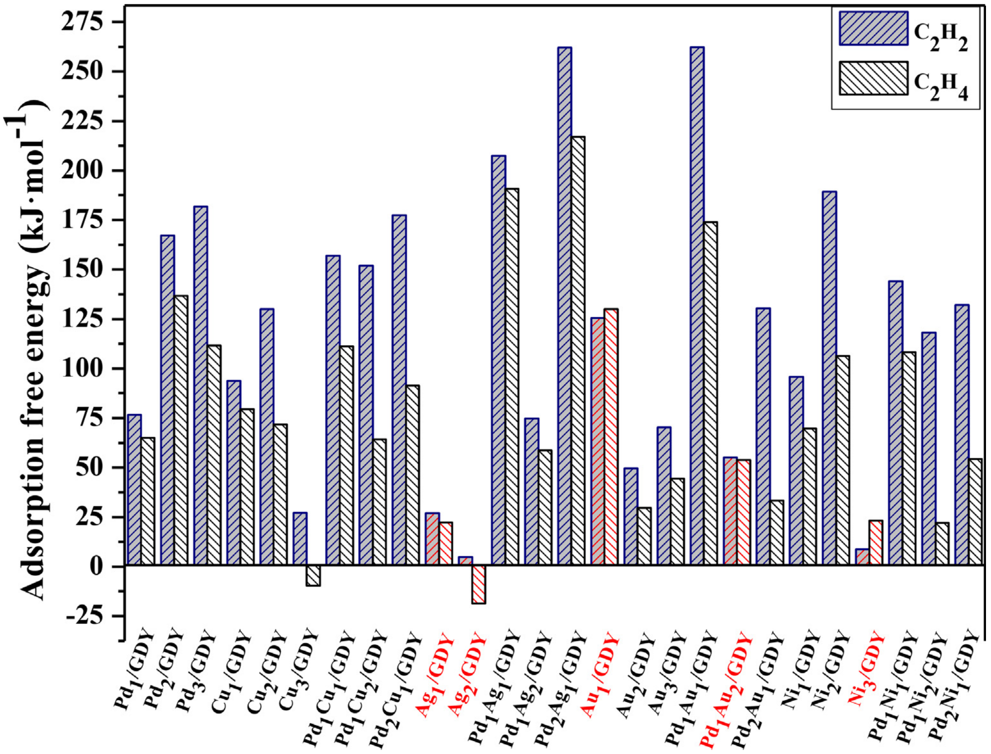

Fig. 4. C_2H_2 and C_2H_4 adsorption free energies on the Pd_xM_y/GDY catalysts at 425 K.

C_2H_2 physisoption or the close adsorption ability between C_2H_2 and C_2H_4 species. Further, on other twenty-one kinds of Pd_xM_y/GDY catalysts, C_2H_2 has stronger adsorption than C_2H_4, which favors the hydrogenation of C_2H_2.

3.3. The priority of C_2H_4 between its desorption and hydrogenation

For Pd_xM_y/GDY catalysts with stronger adsorption ability of C_2H_2 than C_2H_4, it is needed to firstly identify the priority of C_2H_4 between its desorption and hydrogenation, as listed in Table 1 (see the structures in Fig. S3).

For Pd_xM_y/GDY catalysts, C_2H_4+H→C_2H_5 is more favored or competitive compared to C_2H_4 desorption on the Pd_2/GDY, Pd_3/GDY, Cu_1/GDY, Pd_1Cu_1/GDY, Pd_1Ag_1/GDY, Pd_2Ag_1/GDY, Pd_1Au_1/GDY and Ni_1/GDY catalysts, which easily leads to ethane, thus, these eight kinds of Pd_xM_y/GDY catalysts exhibit poor C_2H_4 selectivity, $CHCH_3$ hydrogenation route does not need to be considered. However, as listed in Table 1, C_2H_4 desorption would be superior to its hydrogenation to C_2H_5 on thirteen kinds of Pd_xM_y/GDY catalysts, including Pd_1/GDY, Cu_2/GDY, Cu_3/GDY, Pd_1Cu_2/GDY, Pd_2Cu_1/GDY, Pd_1Ag_2/GDY, Au_2/GDY, Au_3/GDY, Pd_2Au_1/GDY, Ni_2/GDY, Pd_1Ni_1/GDY, Pd_1Ni_2/GDY and Pd_2Ni_1/GDY, which would be favor C_2H_2 semi-hydrogenation to gaseous C_2H_4, and suppress its over-hydrogenation to ethane.

3.4. C_2H_2 semi-hydrogenation on Pd_xM_y/GDY catalysts

As mentioned above, C_2H_4 preferred to be desorption instead of its hydrogenation on thirteen kinds of Pd_xM_y/GDY catalysts, namely, C_2H_4 desorption route become dominant

Table 1
The activation barrier (G_a/$kJ\cdot mol^{-1}$) and reaction energy (ΔG/$kJ\cdot mol^{-1}$) of C_2H_4 hydrogenation to C_2H_5, C_2H_4 desorption free energy of (G_{des}/$kJ\cdot mol^{-1}$) on the Pd_xM_y/GDY catalysts at 425 K.

Catalysts	G_a	ΔG	$G_{des(C2H4)}$	Catalysts	G_a	ΔG	$G_{des(C2H4)}$
Pd_1/GDY	326.5	−37.2	65.1	Au_2/GDY	413.8	2.1	29.6
Pd_2/GDY	68.5	−13.2	136.7	Au_3/GDY	98.6	−38.1	44.5
Pd_3/GDY	95.8	−19.6	111.6	Pd_1Au_1/GDY	24.4	−83.1	173.9
Cu_1/GDY	42.9	−65.1	79.5	Pd_2Au_1/GDY	138.0	10.4	33.3
Cu_2/GDY	186.4	−12.9	71.9	Ni_1/GDY	21.4	−29.9	69.8
Cu_3/GDY	153.0	23.7	−9.6	Ni_2/GDY	182.0	−51.5	106.3
Pd_1Cu_1/GDY	99.1	−30.4	111.2	Pd_1Ni_1/GDY	116.6	3.5	108.2
Pd_1Cu_2/GDY	373.4	12.4	64.3	Pd_1Ni_2/GDY	107.6	23.2	22.1
Pd_2Cu_1/GDY	158.5	−5.2	91.4	Pd_2Ni_1/GDY	204.9	11.9	54.4
Pd_1Ag_1/GDY	9.0	−64.9	190.8				
Pd_1Ag_2/GDY	77.9	28.9	58.6				
Pd_2Ag_1/GDY	156.1	16.0	217.1				

Please cite this article as: Y. Wang et al., C_2H_2 semi-hydrogenation on the Pd_xM_y cluster/graphdiyne catalysts: Effects of cluster composition and size on the activity and selectivity, Green Energy & Environment, https://doi.org/10.1016/j.gee.2020.10.020

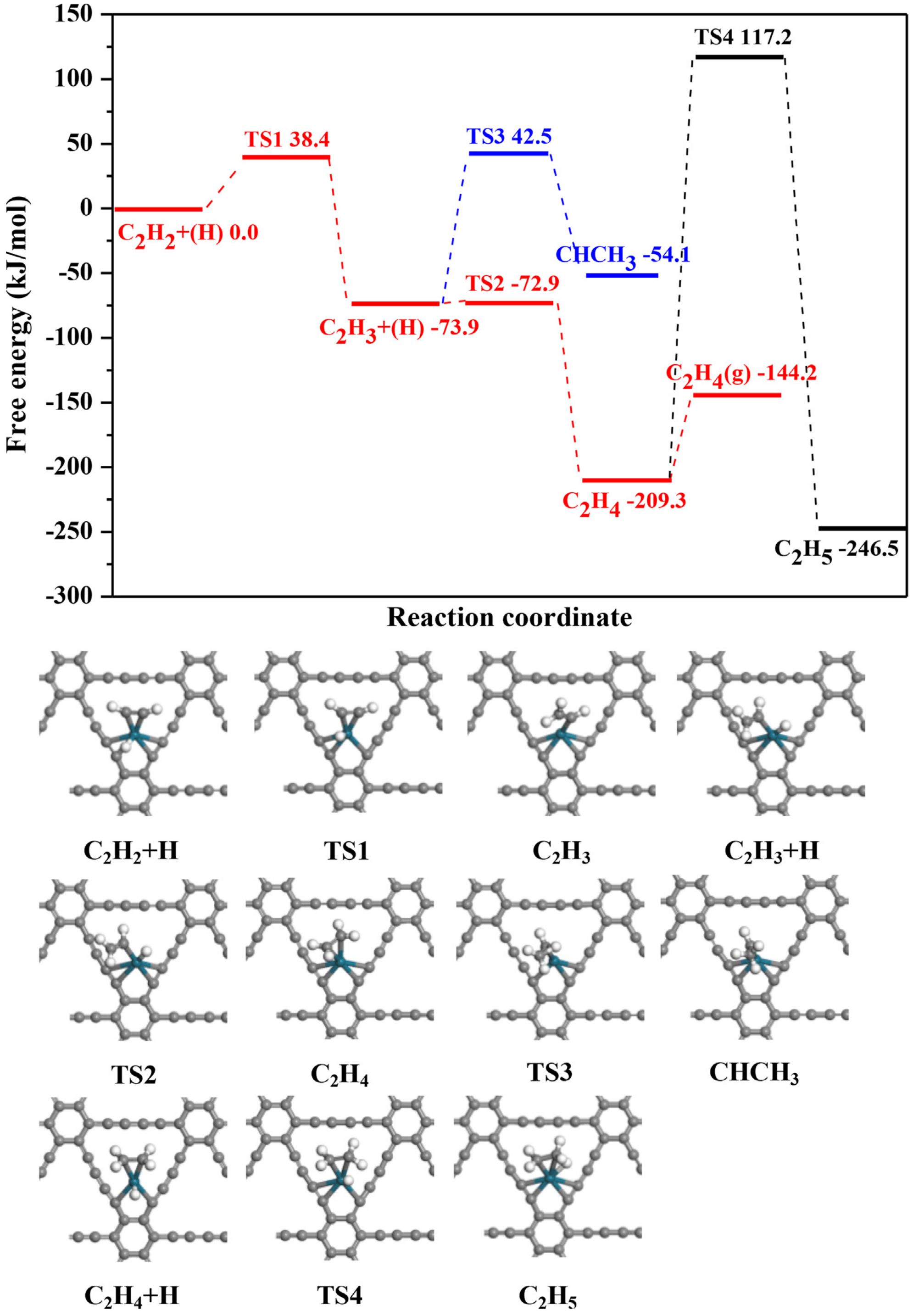

Fig. 5. The energy profiles for three routes of C_2H_2 semi-hydrogenation along with the structures of initial states, transition states and final states on Pd_1/GDY catalyst.

compared to C_2H_4 hydrogenation route, thus, we need to further identify whether C_2H_4 desorption route also prefers to occur compared to $CHCH_3$ hydrogenation route on these thirteen kinds of Pd_xM_y/GDY catalysts (see details in Figs. S4–S15). The energy profiles of C_2H_2 semi-hydrogenation on Pd_1/GDY catalyst is shown in Fig. 5 as an example.

On Pd_1/GDY catalyst, C_2H_2+H→C_2H_3 has the activation barrier of 38.4 kJ mol^{-1}, and it is exothermic by 73.9 kJ mol^{-1}; starting from C_2H_3 intermediate, C_2H_4 formation is superior to $CHCH_3$ formation in kinetics (1.0 *vs.* 116.4 kJ mol^{-1}); further, C_2H_4 desorption would be much preferred kinetically compared to C_2H_4+H→C_2H_5 (65.1 *vs.* 326.5 kJ mol^{-1}), suggesting that Pd_1/GDY catalyst is in favor of C_2H_2 semi-hydrogenation to produce gaseous C_2H_4. Similarly, the easy formation of gaseous C_2H_4 also occurs on the Cu_2/GDY (Fig. S4), Cu_3/GDY (Fig. S5), Pd_1Cu_2/GDY (Fig. S6), Pd_2Cu_1/GDY (Fig. S7), Pd_1Ag_2/GDY (Fig. S8), Au_2/GDY (Fig. S9), Au_3/GDY (Fig. S10), Pd_2Au_1/GDY

Please cite this article as: Y. Wang et al., C_2H_2 semi-hydrogenation on the Pd_xM_y cluster/graphdiyne catalysts: Effects of cluster composition and size on the activity and selectivity, Green Energy & Environment, https://doi.org/10.1016/j.gee.2020.10.020

(Fig. S11) and Pd_1Ni_2/GDY catalysts (Fig. S14). However, $CHCH_3$ formation leading to ethane is much easier than C_2H_4 formation on the Ni_2/GDY (Fig. S12, 62.0 and 105.7 kJ mol^{-1}), Pd_1Ni_1/GDY (Fig. S13, 70.3 and 137.9 kJ mol^{-1}) and Pd_2Ni_1/GDY catalysts (Fig. S15, 40.9 and 115.2 kJ mol^{-1}), as a result, these three types of catalysts present poor C_2H_4 selectivity due to the formation of ethane.

3.5. Selectivity and activity of C_2H_2 semi-hydrogenation on Pd_xM_y/GDY catalysts

The energy difference between C_2H_4 hydrogenation and its adsorption was used to quantitatively describe the selectivity of C_2H_4 (ΔG_s) using the Eq. (1), which has been widely applied in many previous studies [6,28,60,61].

$$\Delta G_s = \Delta G_a - |G_{ads}| \tag{1}$$

Where G_{ads} and ΔG_a correspond to C_2H_4 adsorption free energy and the activation barrier of C_2H_4 hydrogenation to C_2H_5, respectively; the positive and large value of ΔG_{sel} means that the catalyst exhibits better C_2H_4 selectivity. As mentioned above, ten kinds of Pd_xM_y/GDY catalysts have better C_2H_4 selectivity, including Pd_1/GDY, Cu_2/GDY, Cu_3/GDY, Pd_1Cu_2/GDY, Pd_2Cu_1/GDY, Pd_1Ag_2/GDY, Au_2/GDY, Au_3/GDY, Pd_2Au_1/GDY and Pd_1Ni_2/GDY.

Meanwhile, according to the two-step model widely used in the previous work [56,58,62,63] (see details in the Supplementary Material), the reaction rate of C_2H_4 formation was calculated to evaluate the catalytic activity on these ten kinds of Pd_xM_y/GDY catalysts.

As listed in Table 2, the selectivity of C_2H_4 over ten kinds of Pd_xM_y/GDY catalysts, Pd_1/GDY, Cu_2/GDY, Cu_3/GDY, Pd_1Cu_2/GDY, Pd_2Cu_1/GDY, Pd_1Ag_2/GDY, Au_2/GDY, Au_3/GDY, Pd_2Au_1/GDY and Pd_1Ni_2/GDY, are 261.4, 114.5, 162.6, 309.1, 67.1, 19.3, 384.2, 54.1, 104.7 and 85.5 kJ mol^{-1}, respectively, the corresponding activity of C_2H_4 formation are 1.69×10^8, 2.94×10^6, 7.63×10^{-4}, 3.45×10^{-1}, 3.45×10^{-1}, 4.25×10^9, 1.55×10^8, 8.71×10^{-28}, 2.16×10^{-1}, 2.26×10^7 and 3.63×10^{10} $s^{-1}\cdot site^{-1}$, respectively.

Table 2
The values of G_R^{ad}-G_R^{de}+G_P^{de}, G_P^{de} (kJ·mol^{-1}), C_2H_4 selectivity (ΔG_s/kJ mol^{-1}), C_2H_4 formation rate (r/$s^{-1}\cdot site^{-1}$) and average Bader charge (e) for Pd atoms or M atoms in C_2H_2 semi-hydrogenation on the Pd_xM_y/GDY catalysts at 425 K.

Catalysts	G_R^{ad}-G_R^{de}+G_P^{de}	G_P^{de}	ΔG_s	r	e
Pd_1/GDY	−23.7	38.4	261.4	1.69×10^8	0.277
Cu_2/GDY	44.9	31.6	114.5	2.94×10^6	0.387
Cu_3/GDY	95.7	130.7	162.6	7.63×10^{-4}	0.349
Pd_1Cu_2/GDY	−2.3	109.1	309.1	3.45×10^{-1}	0.112
Pd_2Cu_1/GDY	−97.5	27.0	67.1	4.25×10^9	0.177
Pd_1Ag_2/GDY	−12.5	38.7	19.3	1.55×10^8	0.148
Au_2/GDY	317.7	285.3	384.2	8.71×10^{-28}	0.032
Au_3/GDY	100.	108.0	54.1	2.16×10^{-1}	0.135
Pd_2Au_1/GDY	37.7	8.7	104.7	2.26×10^7	0.228
Pd_1Ni_2/GDY	−0.4	19.3	85.5	3.63×10^{10}	0.156

Further, H_2 dissociation may affect the activity of C_2H_4 formation; H_2 adsorption and dissociation were calculated on above ten kinds of Pd_xM_y/GDY catalysts with better C_2H_4 selectivity (see Table S4 and Fig. S19). Our results show that only on the Au_3/GDY, Pd_2Au_1/GDY and Pd_1Ni_2/GDY catalysts, the activation free energies of the rate-determining in C_2H_4 desorption route is lower than those of H_2 dissociation, namely, H_2 dissociation affects the catalytic activity toward C_2H_2 semi-hydrogenation to C_2H_4. Whereas it does not affect the catalytic activity of C_2H_4 formation on other seven types of Pd_1/GDY, Cu_2/GDY, Cu_3/GDY, Pd_1Cu_2/GDY, Pd_2Cu_1/GDY, Pd_1Ag_2/GDY and Au_2/GDY catalysts. Moreover, since this study only focus on the investigations about the effect of active metal types including the metal cluster composition and size on activity and selectivity of C_2H_2 semi-hydrogenation process, the effect of the initial H_2 dissociation activity on the catalytic performance of C_2H_2 semi-hydrogenation process will be considered in our next work.

3.6. General discussions

3.6.1. The effects of cluster composition and size on C_2H_4 formation

For GDY supported single-metal catalysts, firstly, when the supported metal is the single atom, only Pd_1/GDY is favorable for C_2H_4 formation, while on the Cu_1/GDY, Ag_1/GDY, Au_1/GDY and Ni_1/GDY, C_2H_2 could not be effectively adsorbed or the over-hydrogenation of C_2H_4 to ethane occurs. Secondly, when the supported metal is the double and three atoms cluster, only the Cu and Au clusters (Cu_2/GDY, Cu_3/GDY, Au_2/GDY, Au_3/GDY) are favorable for C_2H_4 formation; while on the Pd, Ag and Ni clusters, C_2H_2 cannot be effectively adsorbed or C_2H_4 is inclined to be over-hydrogenated to ethane. Thus, only five kinds of single metal catalysts including Pd_1/GDY, Cu_2/GDY, Cu_3/GDY, Au_2/GDY and Au_3/GDY are favorable for C_2H_2 semi-hydrogenation to form gas phase C_2H_4.

For GDY supported bimetallic catalysts, firstly, when the supported metal is double atoms cluster, all catalysts including Pd_1Cu_1/GDY, Pd_1Ag_1/GDY, Pd_1Au_1/GDY, Pd_1Ni_1/GDY are not favorable for C_2H_2 semi-hydrogenation to C_2H_4. However, when the supported metal is three atoms cluster, only five kinds of the catalysts including Pd_1Cu_2/GDY, Pd_2Cu_1/GDY, Pd_1Ag_2/GDY, Pd_2Au_1/GDY and Pd_1Ni_2/GDY are favorable for C_2H_2 semi-hydrogenation to C_2H_4.

Fig. 6 shows C_2H_4 selectivity and its formation activity over ten kinds of Pd_xM_y/GDY catalysts favored the formation of gaseous C_2H_4 (Pd_1/GDY, Cu_2/GDY, Cu_3/GDY, Pd_1Cu_2/GDY, Pd_2Cu_1/GDY, Pd_1Ag_2/GDY, Au_2/GDY, Au_3/GDY, Pd_2Au_1/GDY and Pd_1Ni_2/GDY), among them, the catalysts with high C_2H_4 selectivity are Au_2/GDY (384.2 kJ mol^{-1}), Pd_1Cu_2/GDY (309.1 kJ mol^{-1}), Pd_1/GDY (261.4 kJ mol^{-1}) and Cu_3/GDY (162.6 kJ mol^{-1}), accordingly, C_2H_4 formation activity are 8.71×10^{-28}, 3.45×10^{-1}, 1.69×10^8 and 7.63×10^{-4} s^{-1}·$site^{-1}$, respectively, indicating that Pd_1/GDY has the highest C_2H_4 formation activity, while Au_2/GDY, Pd_1Cu_2/GDY and Cu_3/GDY presents poor C_2H_4 formation

Please cite this article as: Y. Wang et al., C_2H_2 semi-hydrogenation on the Pd_xM_y cluster/graphdiyne catalysts: Effects of cluster composition and size on the activity and selectivity, Green Energy & Environment, https://doi.org/10.1016/j.gee.2020.10.020

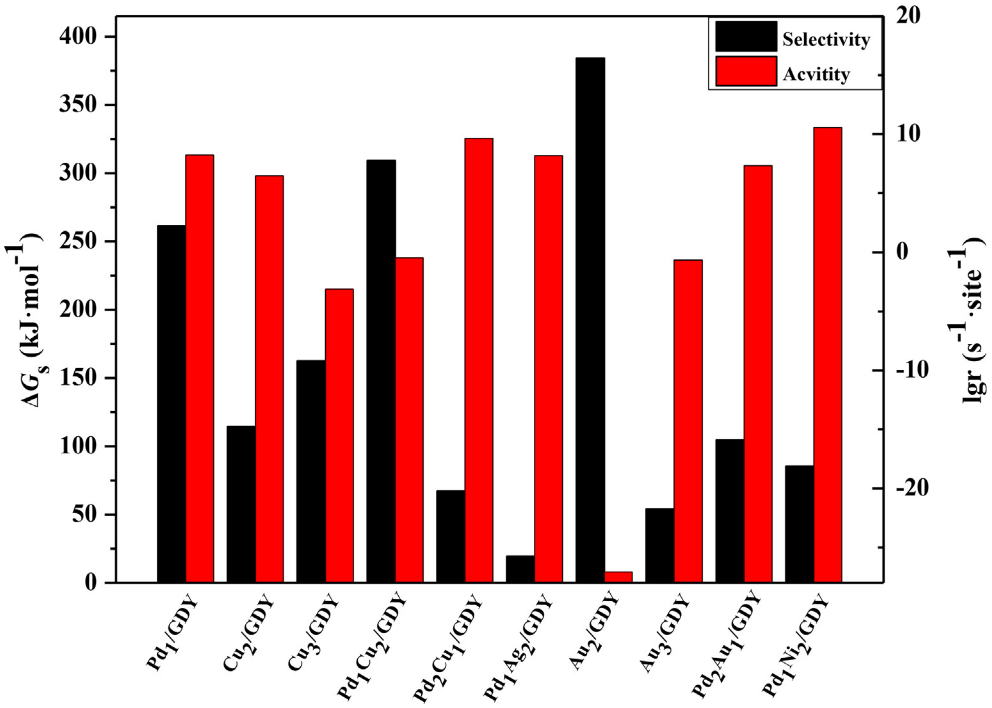

Fig. 6. The selectivity and activity of C_2H_4 formation in C_2H_2 semi-hydrogenation on ten kinds of Pd_xM_y/GDY catalysts to form gaseous C_2H_4 at 425 K.

activity. On the other hand, the catalysts with high C_2H_4 formation activity are Pd_1Ni_2/GDY (3.63 × 10^{10} s^{-1}·$site^{-1}$), Pd_2Cu_1/GDY (4.25 × 10^9 s^{-1}·$site^{-1}$), Pd_1/GDY (1.69 × 10^8 s^{-1}·$site^{-1}$) and Pd_1Ag_2/GDY (1.55 × 10^8 s^{-1}·$site^{-1}$), accordingly, C_2H_4 selectivity are 85.5, 67.1, 261.4 and 19.3 kJ mol^{-1}, respectively, thus, Pd_1/GDY catalyst presents the highest C_2H_4 selectivity. As shown in Fig. S20, generally, there is not a seesaw effect for the activity and selectivity, only both Au_2/GDY and Pd_1Cu_2/GDY have higher C_2H_4 selectivity (384.2 and 309.1 kJ mol^{-1}), while these two catalysts have lower activity (8.71 × 10^{-28} and 3.45 × 10^{-1} s^{-1}·$site^{-1}$). On the contrary, Pd_1Ni_2/GDY, Pd_2Cu_1/GDY and Pd_1Ag_2/GDY catalysts have higher activity of C_2H_4 formation (3.63 × 10^{10}, 4.25 × 10^9 and 1.55 × 10^8 s^{-1}·$site^{-1}$), while the lower C_2H_4 selectivity (85.5, 67.1 and 19.3 kJ mol^{-1}).

Based on above analysis, the composition and size of supported metal cluster Pd_xM_y in Pd_xM_y/GDY catalysts present the sensitivity toward the selectivity and activity of C_2H_2 semi-hydrogenation. Among them, taking C_2H_4 selectivity and its formation activity into consideration, GDY supported single atom Pd catalyst (Pd_1/GDY) in this study should provide the best selectivity (261.4 kJ mol^{-1}) and excellent catalytic activity (1.69 × 10^8 s^{-1}·$site^{-1}$) for C_2H_2 semi-hydrogenation to gaseous C_2H_4.

Further, the catalytic origin of Pd_1/GDY catalyst with the highest activity is revealed. The high C_2H_4 selectivity should be attributed to the structural confinement of single atom Pd in Pd_1/GDY leading to the much weaker C_2H_4-π bonding interactions (65.1 kJ mol^{-1}) compared to the stronger C_2H_4 adsorption on the large size of Pd_{55} cluster (189.2 kJ mol^{-1}) [63]. The weaker C_2H_4-π bonding interactions do not facilitate C_2H_4 activation and hydrogenation. The C_3H_6-π bonding characteristics between C_3H_6 and V_1/g-C_3N_4 catalyst were also obtained [64]. As a result, C_2H_4 hydrogenation (326.5 kJ mol^{-1}) is much difficult than C_2H_4 desorption (65.1 kJ mol^{-1}) on Pd_1/GDY catalyst, the produced C_2H_4 will easily desorb from Pd_1/GDY catalyst to become the dominant product. Meanwhile, compared to the large size of metal Pd_{55} cluster, the faster desorption rate of C_2H_4 on Pd_1/GDY catalyst enhances C_2H_4 selectivity.

3.6.2. The analysis of metal-support interaction and electronic properties

As shown in Fig. 7, the metal-support interaction (E_{MSI}/kJ·mol^{-1}) of Pd_xM_y/GDY catalyst showed that when E_{MSI} value was weak (−200~-400 kJ mol^{-1}) or strong (−600~-800 kJ mol^{-1}), for example, Ag_3/GDY (−236.0), Au_1/GDY (−265.5), Ag_2/GDY (−321.5), Pd_1Au_1/GDY (−322.6), Ag_1/GDY (−338.5), Pd_1Au_2/GDY (−381.5), Pd_1Ag_1/GDY (−400.7), Pd_1Ni_1/GDY (−604.0), Ni_2/GDY (−654.4), Pd_3/GDY (−654.8), Pd_2Ni_1/GDY (-667.8) and Ni_3/GDY (-772.1), these catalysts could not adsorb C_2H_2 preferentially or were not conducive to C_2H_4 formation; however, when the values of E_{MSI} were moderate (−400~-600 kJ·mol^{-1}), the catalyst could adsorb C_2H_2 preferentially and realize C_2H_4 formation, for example, Au_3/GDY (-418.3), Cu_2/GDY (-440.6), Pd_1Ag_2/GDY (-463.9), Pd_1/GDY (-481.1), Pd_2Au_1/GDY (-485.5), Pd_1Cu_2/GDY (-561.4) and Pd_2Cu_1/GDY (-595.1) catalysts are all favorable for C_2H_4 production.

As listed in Table 2, Bader charge indicates that the Pd, Cu, Ag, Au or Ni atoms transfer electrons to the C atom of GDY. For Pd_xM_y/GDY with better C_2H_4 selectivity, when the average charge of metal atoms is small, such as Au_2/GDY (0.032), Pd_1Cu_2/GDY (0.112) and Au_3/GDY (0.135), these

Please cite this article as: Y. Wang et al., C_2H_2 semi-hydrogenation on the Pd_xM_y cluster/graphdiyne catalysts: Effects of cluster composition and size on the activity and selectivity, Green Energy & Environment, https://doi.org/10.1016/j.gee.2020.10.020

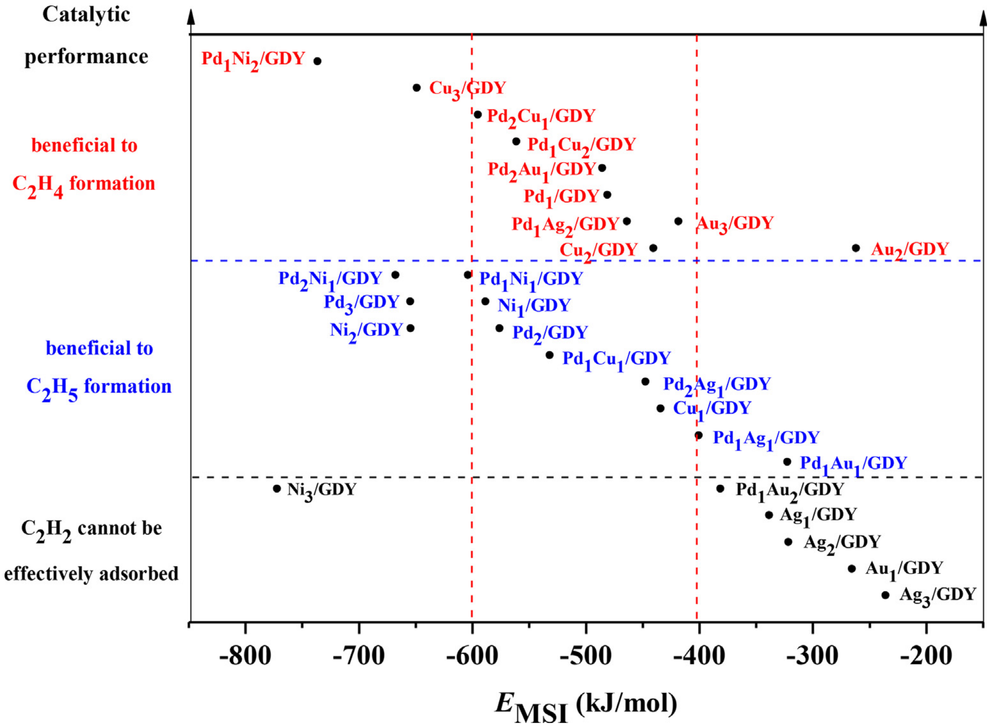

Fig. 7. The effect of the metal-support interaction of Pd_xM_y/GDY catalysts on the activity and selectivity of C_2H_4 formation in C_2H_2 semi-hydrogenation.

catalysts have low C_2H_4 formation activity of 8.71×10^{-28}, 3.45×10^{-1} and 2.16×10^{-1} $s^{-1}\cdot site^{-1}$, respectively. When the average charge of metal atoms is large, such as Cu_3/GDY (0.349) and Cu_2/GDY (0.387), both catalysts also have low C_2H_4 formation activity of 7.63×10^{-4} and 2.94×10^{6} $s^{-1}\cdot site^{-1}$, respectively. Only when the average charge of metal atoms is moderate, such as Pd_1Ag_2/GDY (0.148), Pd_1Ni_2/GDY (0.156), Pd_2Cu_1/GDY (0.177), Pd_2Au_1/GDY (0.228) and Pd_1/GDY (0.277), these catalysts have higher C_2H_4 formation activity of 1.55×10^{8}, 3.63×10^{10}, 4.25×10^{9} and 2.26×10^{7} $s^{-1}\cdot site^{-1}$, respectively. Thus, the average charge amount of metal atom is closely related to C_2H_4 formation activity, namely, the average charge amount of metal atom is less or more, C_2H_4 formation activity is low; whereas the average charge amount of metal atom is moderate, C_2H_4 formation activity is high.

On the other hand, Huang et al. [65] implied that coke formation on the single-atom Pd_1/C_3N_4 is markedly inhibited compared to Pd NP catalysts in C_2H_2 hydrogenation, the geometric effect improved coking-resistance. The oligomerization of C_2H_2 can be avoided on Pd_1/ND@G catalyst, which is attributed to the pyramidal geometry between Pd and C atoms [15]. Indeed, C_2H_2 polymerization to form green oil or coke requires multiple adjacent adsorption sites that cannot be available for Pd single atom, thus, coke formation is suppressed on the Pd single atoms compared to that on the Pd NP catalyst. Similarly, Pd_1/GDY catalyst in the present study only has a single active site, which can suppress the green oil or coke formation due to its unique geometric effect. Further, previous DFT studies [6] have revealed that Pd (111) with surface or subsurface C atom make the shift of the *d*-projected density of states of the surface Pd atoms to lower energy level, which weakens C_2H_4 adsorption compared to those on clean Pd (111) surface, meanwhile, the activity of Pd (111) surface slightly increase in the presence of subsurface carbon species. As a result, C_2H_4 desorption becomes easier, and the selectivity of C_2H_4 increase in the presence of surface and subsurface carbon. The projected density of states (*p*DOS) plots for the *d*-orbitals of Pd atom on the Pd (111)-surface C, Pd (111)-subsurface C, Pd_1/GDY and Pd (111) catalysts are calculated, as shown in Fig. S21, similar to Pd (111) in the presence of surface or subsurface carbon species, compared to the pure Pd (111) surface, the shift of the *d*-projected density of states for surface Pd atoms to lower energy level also occur on Pd_1/GDY, which also weaken C_2H_4 adsorption to increases its selectivity.

3.6.3. The comparisons of catalytic performance between Pd_1/GDY and the previously reported catalysts

To deeply illustrate the excellent activity and selectivity of Pd_1/GDY catalyst, the comparisons for the activity and selectivity of C_2H_4 formation between Pd_1/GDY and the reported catalysts in the literatures were carried out. On Pd_1/GDY catalyst, C_2H_4 selectivity was 261.4 kJ mol^{-1}, both $C_2H_2+H \rightarrow C_2H_3$ and $C_2H_3+H \rightarrow C_2H_4$ reactions have the activation barriers of 36.0 and 1.0 kJ mol^{-1}, respectively; the overall barrier of $C_2H_2+2H \rightarrow C_2H_4$ was 38.4 kJ$\cdot mol^{-1}$.

As shown in Fig. 8(a), for the Pd-based intermetallic compounds (IMCs), the single atom Pd active site can be completely isolated by the second metal, Zhou et al. [66]

Please cite this article as: Y. Wang et al., C_2H_2 semi-hydrogenation on the Pd_xM_y cluster/graphdiyne catalysts: Effects of cluster composition and size on the activity and selectivity, Green Energy & Environment, https://doi.org/10.1016/j.gee.2020.10.020

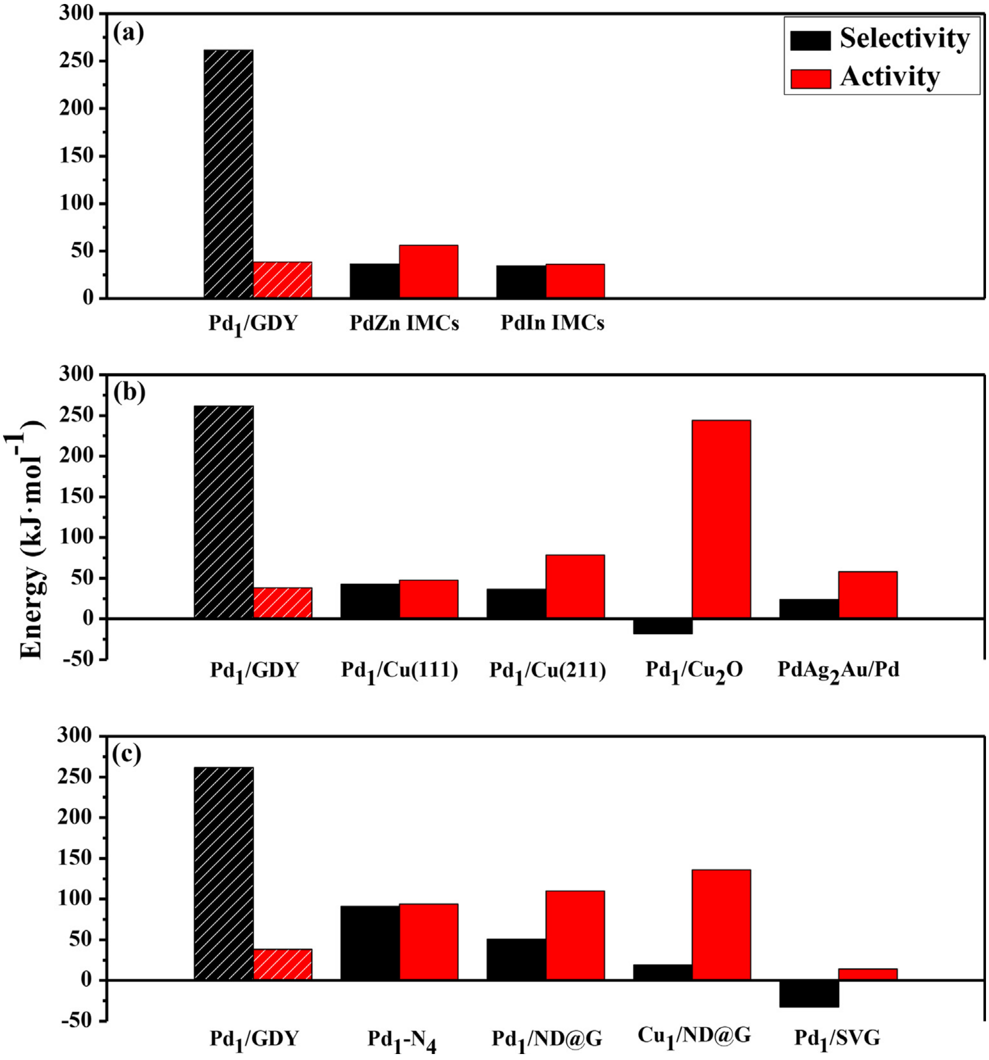

Fig. 8. Comparisons for the activity and selectivity of C_2H_4 formation between Pd_1/GDY and other previously reported single atom Pd or Cu catalysts (a) Intermetallic compounds, (b) surface alloys (C) the supported catalysts in C_2H_2 semi-hydrogenation. The black bar stands for C_2H_4 selectivity, and the red bar stands for the overall barrier of C_2H_4 formation to reflect the activity, respectively. Higher black bar and lower red bar indicates higher C_2H_4 selectivity and its formation activity, respectively.

found that PdZn IMCs had highly active and selective for C_2H_2 semi-hydrogenation, DFT results showed that C_2H_4 selectivity was 36.0 kJ mol^{-1}, meanwhile, the activation barriers of C_2H_2+H→C_2H_3 and C_2H_3+H→C_2H_4 were 55.0 and 56.0 kJ mol^{-1}, respectively. Feng et al. [67] found that the single atom Pd active site in PdIn IMCs had C_2H_4 selectivity of 34.0 kJ mol^{-1}; the activation barriers of C_2H_2+H→C_2H_3 and C_2H_3+H→C_2H_4 were 36.0 and 34.0 kJ mol^{-1}, respectively. Sandoval et al. [68] calculated that the activation barriers of C_2H_2+H→C_2H_3 and C_2H_3+H→C_2H_4 on PdGa IMCs were 70.0 and 75.0 kJ mol^{-1}, respectively. Hence, compared to Pd_1/GDY catalyst in this study, the activity and selectivity of C_2H_4 formation over these reported Pd-based IMCs catalysts are lower.

As shown in Fig. 8(b), for the single atom Pd doped into metal surface, Zhang et al. [57,58] studied the hydrogenation of C_2H_2 on the single atom Pd-doped Cu(111), Cu(211) or Cu_2O(111) surfaces, C_2H_4 selectivity and the overall activation barrier of C_2H_2+2H→C_2H_4 on Pd_1/Cu(111) are 42.6 and 47.5 kJ·mol^{-1}, respectively; those on Pd_1/Cu(211) are 36.4 and 78.8 kJ·mol^{-1}, respectively; on Pd_1/Cu_2O(111), C_2H_2 is easily over-hydrogenated to ethane via $CHCH_3$ intermediate. On the other hand, for the single Pd atom doped-Cu_{13}, Cu_{38} or Cu_{55} clusters [69], C_2H_4 is easily hydrogenated to ethane. Wang et al. [70] obtained that the single atom Pd-doped Ag surface can facilitate the over-hydrogenation of C_2H_4 to produce ethane. Yang et al. [6] found that when the surface coverage of Cu, Ag or Au on Pd (111) is increased to present the single atom Pd, C_2H_4 was prone to be over-hydrogenated to ethane. Yang et al. [71] showed that trimetallic $PdAg_2Au$/Pd (111) surface showed C_2H_4 selectivity of 24.0 kJ·mol^{-1}, the activation barriers of C_2H_2+H→C_2H_3 and C_2H_3+H→C_2H_4 were 41.0 and 58.0 kJ·mol^{-1}, respectively. Thus, the selectivity and activity of C_2H_4 formation over the catalysts doping the single atom Pd into metal surface are still lower than those on Pd_1/GDY catalyst.

As shown in Fig. 8(c), for the supported single atom Pd catalysts, Wei et al. [72] experimentally prepared the

Please cite this article as: Y. Wang et al., C_2H_2 semi-hydrogenation on the Pd_xM_y cluster/graphdiyne catalysts: Effects of cluster composition and size on the activity and selectivity, Green Energy & Environment, https://doi.org/10.1016/j.gee.2020.10.020

thermodynamically stable Pd_1–N_4 structure with the single atom Pd anchored on the defects of nitrogen-doped carbon, then, DFT results show that C_2H_4 selectivity is 91.0 kJ·mol^{-1}; the activation barriers of C_2H_2 hydrogenation and C_2H_3 hydrogenation are 37.0 and 94.0 kJ·mol^{-1}, respectively. The experiments by Huang et al. [15] prepared the atomically dispersed Pd over a defective nanodiamond-graphene (Pd_1/ND@G catalyst), DFT results show that C_2H_4 selectivity is 51.0 kJ·mol^{-1}; the activation barriers of $C_2H_2+H \rightarrow C_2H_3$ and $C_2H_3+H \rightarrow C_2H_4$ are 110.0 and 85.0 kJ·mol^{-1}, respectively. Huang et al. [13] experimentally prepared Cu_1/ND@G catalyst, which also exhibits excellent catalytic performance for $C_2H_2+2H \rightarrow C_2H_4$, and DFT results show that C_2H_4 selectivity is only 19.0 kJ·mol^{-1}; the activation barrier of C_2H_2 hydrogenation to C_2H_3 is 136.0 kJ·mol^{-1}. Zhou et al. [73] found that atomically dispersed Pd on nitrogen-doped graphene (Pd_1/N-graphene) exhibits better activity and selectivity for $C_2H_2+2H \rightarrow C_2H_4$, and DFT results show that C_2H_4 selectivity is 88.0 kJ·mol^{-1}, which is much lower than that on Pd_1/GDY catalyst. Further, C_2H_2 semi-hydrogenation on the Pd_1/SVG catalyst with the single atom Pd supported by a single vacancy graphene (SVG) is calculated in this study (see details in Figs. S16 and S17), the results show that C_2H_4 is easily over-hydrogenated to C_2H_5 in kinetically instead of its desorption (10.6 *vs*. 43.2 kJ mol^{-1}). Similarly, the selectivity and activity of C_2H_4 formation over these supported single atom Pd catalysts reported in the literatures are still lower than those on Pd_1/GDY catalyst.

Based on above analysis, surprisingly, we found that GDY supported single atom Pd catalyst (Pd_1/GDY) in this study should so far provide the best selectivity and activity toward C_2H_4 formation in C_2H_2 semi-hydrogenation in comparison with other types of the single atom Pd or Cu catalysts previously reported in the literatures. Moreover, the experiments by Qi et al. [74] found that the direct oxidation–reduction reaction of GDY and $PdCl_4^{2-}$ could realize the chemical deposition of Pd nanoparticles on GDY, which provided an important guidance for the preparation of GDY supported single atom Pd catalyst in the experiment.

4. Conclusions

In summary, the activity and selectivity of a series of the designed Pd_xM_y (M = Cu, Ag, Au, Ni; x+y = 1–3) clusters anchored on GDY (Pd_xM_y/GDY catalysts) in C_2H_2 semi-hydrogenation have been fully examined using DFT calculations. Our results show that the activity and selectivity of C_2H_4 formation in C_2H_2 semi-hydrogenation on the Pd_xM_y/GDY catalysts strongly depend on the composition and size of supported metal cluster, which has the relationship with the metal-support interaction of Pd_xM_y/GDY catalysts and electronic properties. The supported metal is single atom, only Pd_1/GDY is favorable for C_2H_4 formation; the supported metal is two atoms cluster, only Cu_2/GDY and Au_2/GDY are favorable for C_2H_4 formation; the supported metal is three atoms cluster, seven kinds of the catalysts including Cu_3/GDY, Au_3/GDY, Pd_1Cu_2/GDY, Pd_2Cu_1/GDY, Pd_1Ag_2/GDY, Pd_2Au_1/GDY and Pd_1Ni_2/GDY are favorable for C_2H_4 formation. Moreover, aiming at realizing the balance between the activity and selectivity of C_2H_4 formation, the metal-support interaction of Pd_xM_y/GDY catalysts and the average charge amount of metal atoms should be maintain in a moderate range.

Surprisingly, the comparisons among the catalysts considered in this study and previously reported in the literature showed for the first time that Pd_1/GDY catalyst exhibits the high catalytic activity and selectivity toward C_2H_4 formation in C_2H_2 semi-hydrogenation. The high activity of Pd_1/GDY is ascribed to Pd inherent properties toward C_2H_2 hydrogenation, however, the high C_2H_4 selectivity is attributed to the structural confinement of single atom Pd in Pd_1/GDY catalyst leading to the much weaker C_2H_4-π bonding interactions, which is not favorable for C_2H_4 activation and hydrogenation, thus, the faster desorption rate of the produced C_2H_4 on Pd_1/GDY catalyst than its hydrogenation rate enhanced C_2H_4 selectivity in C_2H_2 semi-hydrogenation. The obtained results could provide good clues for designing and screening out the potential catalysts with GDY supported small sizes of metal clusters for selective hydrogenation of alkanes.

Conflict of interest

The authors declare that they have no known competing financial interests or personal relationships that could have appeared to influence the work reported in this paper.

Acknowledgment

This work is financially supported by the National Natural Science Foundation of China (No. 21776193 and 21736007) and U.S. NSF-sponsored NCAR-Wyoming Supercomputing Center (NWSC).

Appendix A. Supplementary data

Supplementary data to this article can be found online at https://doi.org/10.1016/j.gee.2020.10.020.

References

[1] A. Borodziński, G.C. Bond, Catal. Rev. Sci. Eng. 48 (2006) 91–144.
[2] A. Borodziński, G.C. Bond, Catal. Rev. Sci. Eng. 50 (2008) 379–469.
[3] F. Studt, F. Abild-Pedersen, T. Bligaard, R.Z. Sørensen, C.H. Christensen, J.K. Nørskov, Angew. Chem. Int. Ed. 47 (2008) 9299–9302.
[4] D. Teschner, J. Borsodi, A. Wootsch, Z. Révay, M. Hävecker, A. Knop-Gericke, S.D. Jackson, R. Schlögl, Science 320 (2008) 86–89.
[5] F. Studt, F. Abild-Pedersen, T. Bligaard, R.Z. Sørensen, C.H. Christensen, J.K. Nørskov, Science 320 (2008) 1320–1322.
[6] B. Yang, R. Burch, C. Hardacre, G. Headdock, P. Hu, J. Catal. 305 (2013) 264–276.
[7] X. Liu, D. Tian, C. Meng, J. Mol. Struct. 1080 (2015) 105–110.
[8] B. Mercedes, L.P. Antonio, C. Avelino, Acc. Chem. Res. 47 (2014) 834–844.
[9] J.Y. Zhang, Y.C. Deng, X.B. Cai, Y.L. Chen, M. Peng, Z.M. Jia, Z. Jiang, P.J. Ren, S.Y. Yao, J.L. Xie, D.Q. Xiao, X.D. Wen, N. Wang, H.Y. Liu, D. Ma, ACS Catal. 9 (2019) 5998–6005.

Please cite this article as: Y. Wang et al., C_2H_2 semi-hydrogenation on the Pd_xM_y cluster/graphdiyne catalysts: Effects of cluster composition and size on the activity and selectivity, Green Energy & Environment, https://doi.org/10.1016/j.gee.2020.10.020

[10] A.C. Gluhoi, J.W. Bakker, B.E. Nieuwenhuys, Catal. Today 154 (2010) 13–20.
[11] T. Abdollahi, D. Farmanzadeh, Appl. Surf. Sci. 433 (2018) 513–529.
[12] W. Xiao, R. Zeng, L. Cheng, J.W. Wang, L.J. Jiang, L.G. Wang, RSC Adv. 5 (2015) 61861–61867.
[13] F. Huang, Y.C. Deng, Y.L. Chen, X.B. Cai, M. Peng, Z.M. Jia, J.L. Xie, D.Q. Xiao, X.D. Wen, N. Wang, Z. Jiang, H.Y. Liu, D. Ma, Nat. Commun. 10 (2019) 4431.
[14] X.X. Shi, Y. Lin, L. Huang, Z.H. Sun, Y. Yang, X.H. Zhou, E. Vovk, X.Y. Liu, X.H. Huang, M. Sun, S.Q. Wei, J.L. Lu, ACS Catal. 10 (2020) 3495–3504.
[15] F. Huang, Y.C. Deng, Y.L. Chen, X.B. Cai, M. Peng, Z.M. Jia, P.J. Ren, D.Q. Xiao, X.D. Wen, N. Wang, H.Y. Liu, D. Ma, J. Am. Chem. Soc. 140 (2018) 13142–13146.
[16] G. Li, Y. Li, H. Liu, Y. Guo, Y. Li, D. Zhu, Chem. Commun. 46 (2010) 3256–3258.
[17] C.S. Huang, S.L. Zhang, H.B. Liu, Y.J. Li, G.L. Cui, Y.L. Li, Nanomater. Energy 11 (2015) 481–489.
[18] S.L. Zhang, H.B. Liu, C.S. Huang, G.L. Cui, Y.L. Li, Chem. Commun. 51 (2015) 1834–1837.
[19] N.L. Yang, Y.Y. Liu, H. Wen, Z.Y. Tang, H.J. Zhao, Y.L. Li, D. Wang, ACS Nano 7 (2013) 1504–1512.
[20] H. Qiu, M.M. Xue, C. Shen, Z.H. Zhang, W.L. Guo, Adv. Mater. 31 (2019) 1803772.
[21] W.H. Xu, Y.H. Chen, M.X. Song, X.C. Liu, Y.J. Zhao, M.L. Zhang, C.R. Zhang, J. Phys. Chem. C 124 (2020) 8110–8118.
[22] J. Zhong, J. Wang, J.G. Zhou, B.H. Mao, C.H. Liu, H.B. Liu, Y.L. Li, T.K. Sham, X.H. Sun, S.D. Wang, J. Phys. Chem. C 117 (2013) 5931–5936.
[23] X. Qian, H. Liu, C. Huang, S. Chen, L. Zhang, Y. Li, J. Wang, Y. Li, Sci. Rep. 5 (2015) 1–7.
[24] Z.S. Lu, S. Li, P. Lv, C.Z. He, D.W. Ma, Z.X. Yang, Appl. Surf. Sci. 360 (2016) 1–7.
[25] Z.Z. Lin, Q. Wei, X.M. Zhu, Carbon 66 (2014) 504–510.
[26] Z.W. Chen, Z. Wen, Q. Jiang, J. Phys. Chem. C 121 (2017) 3463–3468.
[27] D.H. Xing, C.Q. Xu, Y.G. Wang, J. Li, J. Phys. Chem. C 123 (2019) 10494–10500.
[28] L. Xu, E.E. Stangland, M. Mavrikakis, J. Catal. 362 (2018) 18–24.
[29] T. Abdollahi, D. Farmanzadeh, C. R. Chim. 21 (2018) 484–493.
[30] N. Wongwaranon, O. Mekasuwandumrong, P. Praserthdam, J. Panpranot, Catal. Today 131 (2008) 553–558.
[31] Q. Jin, Y.F. He, M.Y. Miao, C.Y. Guan, Y.Y. Du, J.T. Feng, D.Q. Li, Appl. Catal. Gen. 500 (2015) 3–11.
[32] B. Delley, J. Chem. Phys. 92 (1990) 508–517.
[33] B. Delley, J. Chem. Phys. 113 (2000) 7756–7764.
[34] B. Hammer, L.B. Hansen, J.K. Nørskov, Phys. Rev. B 59 (1999) 7413–7421.
[35] J.P. Perdew, K. Burke, M. Ernzerhof, Phys. Rev. Lett. 77 (1996) 3865–3868.
[36] A. Bergner, M. Dolg, W. Küchle, H. Stoll, H. Preuß, Mol. Phys. 80 (1993) 1431–1441.
[37] P. Hohenberg, W. Kohn, Phys. Rev. B 136 (1964) B864–B871.
[38] T. Björkman, A. Gulans, A.V. Krasheninnikov, R.M. Nieminen, Phys. Rev. Lett. 108 (2012) 235502.
[39] M. Dolg, U. Wedig, H. Stoll, H. Preuss, J. Chem. Phys. 86 (1987) 866–872.
[40] R.A. Aziz, Mol. Phys. 38 (1979) 177–190.
[41] N. Govind, M. Petersen, G. Fitzgerald, D. King-Smith, J. Andzelm, Comput. Mater. Sci. 28 (2003) 250–258.
[42] T.A. Halgren, W.N. Lipscomb, Chem. Phys. Lett. 49 (1977) 225–232.
[43] Z.J. Zhao, J.B. Zhao, X. Chang, S.J. Zha, L. Zeng, J.L. Gong, AIChE J. 65 (2019) 1059–1066.
[44] J.T. Wehrli, D.J. Thomas, M.S. Wainwright, D.L. Trimm, N.W. Cant, Stud. Surf. Sci. Catal. 68 (1991) 203–210.
[45] I.Y. Ahn, J.H. Lee, S.S. Kum, S.H. Moon, Catal. Today 123 (2007) 151–157.
[46] G.C. Battiston, L. Dalloro, G.R. Tauszik, Appl. Catal. 2 (1982) 1–17.
[47] A. Sárkány, L. Guczi, A.H. Weiss, Appl. Catal. 10 (1984) 369–388.
[48] M. Larsson, J. Jansson, S. Asplund, J. Catal. 178 (1998) 49–57.
[49] A.J. McCue, A.M. Shepherd, J.A. Anderson, Catal. Sci. Technol. 5 (2015) 2880–2890.
[50] A.J. McCue, C.J. McRitchie, A.M. Shepherd, J.A. Anderson, J. Catal. 319 (2014) 127–135.
[51] P. Wu, P. Du, H. Zhang, C. Cai, Phys. Chem. Chem. Phys. 16 (2014) 5640–5648.
[52] Z. Guan, M.F. Xue, Z.Q. Li, R.G. Zhang, B.J. Wang, Appl. Surf. Sci. 503 (2020) 144142.
[53] K. Srinivasu, S.K. Ghosh, J. Phys. Chem. C 117 (2013) 26021–26028.
[54] B. Mattson, W. Foster, J. Greimann, T. Hoette, N. Le, A. Mirich, S. Wankum, A. Cabri, C. Reichenbacher, E. Schwanke, J. Chem. Educ. 90 (2013) 613–619.
[55] U. Schneider, H. Busse, R. Link, G.R. Castro, K. Wandelt, J. Vac. Sci. Technol. 12 (1994) 2069–2073.
[56] B. Zhao, R.G. Zhang, Z.X. Huang, B.J. Wang, Appl. Catal. Gen. 546 (2017) 111–121.
[57] R.G. Zhang, J. Zhang, B. Zhao, L.L. He, A.J. Wang, B.J. Wang, J. Phys. Chem. C 121 (2017) 27936–27949.
[58] R.G. Zhang, B. Zhao, L.L. He, A.J. Wang, B.J. Wang, Phys. Chem. Chem. Phys. 20 (2018) 17487–17496.
[59] W.J. Kim, S.H. Moon, Catal. Today 185 (2012) 2–16.
[60] B. Yang, R. Burch, C. Hardacre, G. Headdock, P. Hu, ACS Catal. 2 (2012) 1027–1032.
[61] M.Z. Hu, W.J. Yang, S.J. Liu, W. Zhu, Y. Li, B.T. Hu, Z. Chen, R.A. Shen, W.-C. Cheong, Y. Wang, K. Zhou, Q. Peng, C. Chen, Y.D. Li, Chem. Sci. 10 (2019) 614–619.
[62] R.G. Zhang, B. Zhao, L.X. Ling, A.J. Wang, C.K. Russell, B.J. Wang, M.H. Fan, ChemCatChem 10 (2018) 2424–2432.
[63] R.G. Zhang, M.F. Xue, B.J. Wang, L.X. Ling, M.H. Fan, J. Phys. Chem. C 123 (2019) 16107–16117.
[64] Y.X. Liu, Y.J. Dong, Z.Y. Tang, X.F. Wang, L. Wang, T.J. Hou, H.P. Lin, Y.Y. Li, J. Mater. Chem. C 4 (2016) 6380–6385.
[65] X.H. Huang, Y.J. Xia, Y.J. Cao, X.S. Zheng, H.B. Pan, J.F. Zhu, C. Ma, H.W. Wang, J.J. Li, R. You, S.Q. Wei, W.X. Huang, J.L. Lu, Nano Res 10 (2017) 1302–1312.
[66] H.R. Zhou, X.F. Yang, L. Li, X.Y. Liu, Y.Q. Huang, X.L. Pan, A.Q. Wang, J. Li, T. Zhang, ACS Catal. 6 (2016) 1054–1061.
[67] Q. Feng, S. Zhao, Y. Wang, J.C. Dong, W. Chen, D. He, D. Wang, J. Yang, Y. Zhu, H. Zhu, L. Gu, Z. Li, Y. Liu, R. Yu, J. Li, Y. Li, Isolated single-atom Pd sites in intermetallic nanostructures: High catalytic selectivity for semi-hydrogenation of alkynes, J. Am. Chem. Soc. 139 (2017) 7294–7301.
[68] M. Sandoval, P. Bechthold, V. Orazi, E.A. González, A. Juan, P.V. Jasen, Appl. Surf. Sci. 435 (2018) 568–573.
[69] R.G. Zhang, M.F. Xue, B.J. Wang, L.X. Ling, Appl. Surf. Sci. 481 (2019) 421–432.
[70] Y. Wang, B.J. Wang, L.X. Ling, R.G. Zhang, M.H. Fan, Chem. Eng. Sci. 218 (2020) 115549.
[71] C.X. Yang, G.Q. Wang, A.M. Liang, Y. Yue, H. Peng, D.J. Cheng, Catal. Commun. 124 (2019) 41–45.
[72] S.J. Wei, A. Li, J.C. Liu, Z. Li, W.X. Chen, Y. Gong, Q.H. Zhang, W.C. Cheong, Y. Wang, L.R. Zheng, H. Xiao, C. Chen, D.S. Wang, Q. Peng, L. Gu, X.D. Han, J. Li, Y.D. Li, Nat. Nanotechnol. 13 (2018) 856–861.
[73] S.Q. Zhou, L. Shang, Y.X. Zhao, R. Shi, G.I.N. Waterhouse, Y.C. Huang, L.R. Zhang, T.R. Zhang, Adv. Mater. 31 (2019) 1900509.
[74] H.T. Qi, P. Yu, Y.X. Wang, G.C. Han, H.B. Liu, Y.P. Yi, Y.L. Li, L.Q. Mao, J. Am. Chem. Soc. 137 (2015) 5260–5263.

Please cite this article as: Y. Wang et al., C_2H_2 semi-hydrogenation on the Pd_xM_y cluster/graphdiyne catalysts: Effects of cluster composition and size on the activity and selectivity, Green Energy & Environment, https://doi.org/10.1016/j.gee.2020.10.020